Journal of Low Temperature Physics, Vol. 17, Nos. 5/6, 1974

The Coupled Phonon Spectrum in ^{3}He–^{4}He Solutions*

David L. Bartley†‡ and Victor K. Wong§**
Department of Physics, University of Michigan, Ann Arbor, Michigan

and John E. Robinson
Argonne National Laboratory, Argonne, Illinois

(Received May 22, 1974)

A simple extension of a model previously used for ^{3}He–^{4}He solutions is presented, in which the effective vertex functions between ^{3}He and ^{4}He density fluctuations are assumed to depend only on the momentum transfer. The possible zero-concentration ^{3}He quasiparticle spectra are divided into two classes, those that do and those that do not intersect the ^{4}He phonon spectrum. The present model calculations of the coupled phonon spectrum demonstrate that as the temperature is decreased the behavior of the shifts in the phonon spectrum can be considered as a signature of the class of ^{3}He quasiparticle spectrum used. Comparison with recent scattering experiments, however, indicates that the existing data are not sufficient to distinguish unambiguously between the two classes of ^{3}He spectrum. It is suggested that a low-temperature neutron scattering experiment be performed to settle this question.

1. INTRODUCTION

In a recent publication[1] (hereafter referred to as I), the present authors have reported a calculation of the density excitation spectrum of the system consisting of a small molar concentration x of ^{3}He atoms dissolved in liquid ^{4}He. The model used consisted of the measured ^{4}He phonon spectrum and the $x = 0$ ^{3}He quasiparticle spectrum, which was assumed to be quadratic in the wave vector k and to intersect the ^{4}He phonon spectrum near the ^{4}He roton wave vector k_4. A simple δ-function interaction between these

*Work supported by the U.S. Atomic Energy Commission.
†Present address: Department of Physics, Brown University, Providence, Rhode Island.
‡Student Associate, Summer 1973, Argonne National Laboratory, Argonne, Illinois.
§Supported in part by a Faculty Research Grant from the Horace H. Rackham School of Graduate Studies at the University of Michigan,
**Faculty Associate, Summer 1973, Argonne National Laboratory, Argonne, Illinois.

bare excitations was assumed, the strength of which was determined by an extrapolation of the phenomenological quantum hydrodynamic value into the short-wavelength regime. As mentioned in I, such an extrapolation is not justified, but was made to illustrate some qualitative features of a renormalized coupled phonon spectrum produced by the interaction between ^{4}He phonons and ^{3}He quasiparticles.

The density excitation spectrum was determined in I for small x by the peaks at $\omega = \omega(k)$ of the ^{4}He dynamic structure function $S(k, \omega)$, taken as a function of the frequency ω at a particular k. Approximating the phonon polarization by a Hartree term and a term involving the virtual decay of a phonon into a quasiparticle–hole pair, we found that the ^{4}He phonon spectrum can be split by the ^{3}He quasiparticle–hole continuum into two distinct branches lying outside the continuum. Similar splittings have been calculated by Soda.[2] We found that the visibility of the splitting of the phonon branches into two branches depended strongly on two physical parameters: (a) the effective coupling γ between the bare excitations near the ^{4}He roton wave vector k_4 and (b) a parameter characterizing the intersection of the assumed ^{3}He quasiparticle spectrum with the measured ^{4}He phonon spectrum. For example, if γ is small enough (i.e., if $\gamma \lesssim 9$ K), the splitting would not be large enough to push the phonon spectrum outside the continuum and a single branch inside the continuum would result. Thus the experimental determination of these physical parameters is important for a quantitative theory.

The recent Raman scattering[3,4] and neutron scattering[5] experiments, which showed shifts in the phonon spectrum only of the order of tenths of a degree, can be used to estimate the order of magnitude of the effective coupling γ near k_4. Without detailed calculations, it is clear that the *caveat* expressed in I was appropriate, namely that the extrapolation of the quantum hydrodynamic value would overestimate the magnitude of γ. From the above experiments we see that γ is overestimated in I by about one order of magnitude (e.g., $\gamma_{\text{exp}} \approx 5$ K). Clearly we need a new calculation of the ^{3}He–^{4}He coupled phonon spectrum that would take into account the smaller value of the effective coupling γ near k_4.

Another recent development concerns the $x = 0$ ^{3}He quasiparticle spectrum. It was proposed by Pitaevski[6] that measurements of the normal fluid density[7] in ^{3}He–^{4}He solutions, which showed an additional exponential dependence on the inverse temperature as x is increased, can be explained in light of the above Raman scattering experiments by the Ansatz that the ^{3}He quasiparticle spectrum exhibits a minimum (in energy as a function of k) that lies below the ^{4}He roton minimum. This Ansatz was supported by a variational calculation by Stephen and Mittag.[8] On the other hand, Bagchi and Ruvalds[9] have proposed that the slight nonlinearity[4] of the roton linewidth

as a function of x is due to the onset of a roton decay process forbidden at small x, and the assumption of a quadratic ^{3}He quasiparticle spectrum intersecting the ^{4}He phonon spectrum is an integral part of the argument. Hence the nature of the ^{3}He quasiparticle spectrum is still unsettled.

The philosophy of I was to calculate the ^{3}He–^{4}He density excitation spectrum in the simplest model consistent with available data. While some relevant microscopic calculations could be performed, e.g., using the method of correlated basis functions, the very extensive numerical work required to address the diversity of temperature- and concentration-dependent effects which appear important is not yet justified by presently available experimental information. Accordingly, in the present work we extend the model used in I in a simple manner so as to accommodate the recent developments. In particular we first replace the δ-function effective interactions by k-dependent vertex functions to take into account the smaller value of γ near k_4. Although effective interactions are described by renormalized vertex functions which are ω dependent also, we consider only the static limit in the interest of simplicity. We then divide the possible ^{3}He quasiparticle spectra into two classes: those that intersect the ^{4}He phonon spectrum and those that do not. To investigate if there exist any qualitative differences between the effects of these two classes of ^{3}He spectra, we calculate the coupled phonon spectrum using a ^{3}He spectrum of each class. We show that further experiments may be able to yield not only detailed information concerning the vertex functions, but also the qualitative features of the large-wavevector part of the ^{3}He quasiparticle spectrum.

In Section 2, we consider the details of the extension of the model used in I, give a brief critique of the use of an effective interaction Hamiltonian, and indicate the approximation used here to calculate the coupled phonon spectrum. In Section 3 we calculate the phonon spectrum using a ^{3}He quasiparticle spectrum of the first class, namely quadratic in k as used in I. We find that at $T = 0$ the shift in the phonon spectrum attains a maximum and minimum which straddle the intersection or crossover wave vector k_c, and that the maximal shifts are of order $x^{2/3}$. In the high-temperature regime, $T \gg T_F$, however, the perturbations become of order x, in both the shift and the increased width of the phonon spectrum. In Section 4 we examine the effect on the phonon spectrum of a particular ^{3}He quasiparticle spectrum of the second class, which is taken to have a minimum below the ^{4}He roton minimum at roughly the same wave vector as k_4. We find a positive contribution to the phonon shift at k_4 which increases markedly with decreasing temperatures. This differs significantly from the low-T effects of intersecting bare spectra, for which the phonon shift near k_4 becomes more negative as the temperature decreases. Finally, in Section 5 we consider the existing experimental scattering data,[3–5] concentrating on the inelastic neutron scattering

experiment because of the direct k-dependent information obtained concerning the density excitations. We show that the existing data are compatible with either class of ^{3}He spectrum. In light of the distinctive temperature dependence of the effects of the two classes of ^{3}He spectra, we suggest a low-temperature neutron scattering experiment, which should be able to ascertain whether the ^{3}He quasiparticle spectrum intersects the ^{4}He phonon spectrum or not.

2. THE MODEL

2.1. The Effective Interaction Hamiltonian

The model used here is a simple extension of the model used in I. A restriction which we impose on the model is that in the long wavelength limit at $T = 0$ it must reduce to the quantum hydrodynamic (QHD) model.[10–12] Following I, we take as the "bare" particles of our model bosons with the measured ^{4}He one-phonon spectrum,[13] $\omega_0(k)$, evaluated at the reduced solution density $n_4 + \delta n_4$ and $T = 0$, and fermions with the $x = 0$ ^{3}He quasiparticle spectrum ε_k in the solution at $T = 0$. In other words, the "bare" components are described by renormalized $T = 0$ propagators but with no background. The ^{4}He background, for example, can then be generated by allowing for a three-phonon vertex. Since we are mainly interested in the coupling between the ^{4}He and ^{3}He spectra, we ignore the above vertex (and thus the backgrounds) and center our attention on the mixed vertices, e.g., on the three-point mixed vertex that involves one phonon and a quasiparticle–hole pair. This phonon–quasiparticle vertex, when renormalized, is generally ω dependent and complex, and as such would not make for a convenient interaction Hamiltonian. To obtain a tractable Hamiltonian, we follow Bardeen, Baym, and Pines[10] (BBP) and assume that the effective vertex, which is taken here as our "bare" vertex, depends only on the difference between the position of the ^{3}He atom at $\mathbf{x}_i$ and the position of the ^{4}He atom at $\mathbf{x}_j$. This assumption effectively excludes any retardation effects or velocity dependence in the "bare" vertex and is equivalent to taking the static and long-wavelength limit of the renormalized vertex in such a way that the vertex depends only on the momentum transfer between the ^{3}He and ^{4}He density fluctuations. The justification of such an assumption lies in the fact that at long wavelengths the typical frequencies of ^{3}He density fluctuations $v_F q$ are much smaller than the typical frequencies of ^{4}He density fluctuations ck. At short wavelengths retardation and velocity-dependent effects may be important and can be included via the vertex corrections. In the QHD model, we find that a mixed four-point vertex describing the scattering of phonons with quasiparticles also appears. We

make the same assumption for the four-point vertex as for the three-point. Since our small parameter is the concentration x, we expect in general the appearance of mixed n-point vertices consisting of a quasiparticle–hole pair with $n-2$ phonons. For simplicity we terminate the infinite series of vertices at $n=4$, as was done in the QHD model. In this manner, we are led to consider the following effective interaction Hamiltonian:

$$\begin{aligned} H_{\text{int}} = & \int d^3x \int d^3x' \left[\gamma_\rho(\mathbf{x}-\mathbf{x}')\rho_3(\mathbf{x},t)\rho_4(\mathbf{x}',t) + \gamma_J(\mathbf{x}-\mathbf{x}')\mathbf{j}_3(\mathbf{x},t)\cdot\mathbf{j}_4(\mathbf{x}',t)\right] \\ & + \int d^3x \int d^3x' \int d^3x'' \\ & \times \left[\tfrac{1}{2}g_\rho(\mathbf{x}-\mathbf{x}',\mathbf{x}-\mathbf{x}'')\rho_3(\mathbf{x},t)\rho_4(\mathbf{x}',t)\rho_4(\mathbf{x}'',t)\right. \\ & \left. + \tfrac{1}{2}g_J(\mathbf{x}-\mathbf{x}',\mathbf{x}-\mathbf{x}'')\rho_3(\mathbf{x},t)\mathbf{j}_4(\mathbf{x}',t)\cdot\mathbf{j}_4(\mathbf{x}'',t)\right] \end{aligned} \tag{1}$$

where $(\rho_3, \mathbf{j}_3)$ and $(\rho_4, \mathbf{j}_4)$ are respectively the ^{3}He and ^{4}He density and current operators given in (6) and (7) of I, $\gamma_\rho(\mathbf{x})$ and $\gamma_J(\mathbf{x})$ are the three-point vertex functions, and $g_\rho(\mathbf{x},\mathbf{x}')$ and $g_J(\mathbf{x},\mathbf{x}')$ are the four-point vertex functions. The basic formalism presented in I is not altered by the use of (1), apart from the fact that the constants γ_ρ, γ_j, g_ρ, and g_J in I must now be replaced by the k-dependent Fourier transforms of the vertex functions in (1).

Some care must be exercised in the use of the perturbation expansion that naturally arises from the effective interaction Hamiltonian (1). Even in the long-wavelength limit, in which (1) becomes the H_{int} used in I, one must be careful if the results of the QHD model are to be recovered. The point is that the effective Hamiltonian $H = H_0 + H_{\text{int}}$ is defined in terms of renormalized propagators and vertices; hence renormalization terms must be excluded to avoid overcounting. A formal exposition of this point for a (pure) Bose liquid at $T=0$ has been presented by Josephson,[14] in which the effective Hamiltonian H used in QHD is accorded the status of a pseudo-Hamiltonian. We can illustrate the anomalous nature of the effective interaction Hamiltonian (1) by comparing the calculation of the x dependence of the sound speed c at $T=0$ with that of the chemical potential ε_0 and effective mass m of ^{3}He atoms dissolved in liquid ^{4}He. The x dependence of $c(x)$ was calculated straightforwardly using the effective Hamiltonian in I [cf. I, (20)–(26)] and was shown to agree with QHD. In the calculations of ε_0 and m, however, an explicit subtraction of a renormalization term must be made before the QHD results can be recovered. Physically, this term is just the self-energy of a single isolated ^{3}He atom dissolved into liquid ^{4}He. The formal distinction between the calculation of $c(x)$ and that of $\varepsilon_0(x)$ and $m(x)$ arises from the fact that the one-loop integral in $c(x)$, which is over fermion lines only, obviously vanishes as $x \to 0$, whereas the one-loop

integral in $\varepsilon_0(x)$ and $m(x)$, which is over a fermion line and a boson line, need not vanish as $x \to 0$. Details of the calculation can be found in Appendix A. Similarly, in calculating temperature corrections, $T = 0$ renormalization terms must be subtracted; in calculating vertex corrections, static long-wavelength renormalization terms must be thrown away; and in calculating the background, renormalization terms that shift the peak of the spectral function must be excluded.

With these provisos, the present model represents a straightforward extension of the QHD model into the short-wavelength regime with allowance for "bare" vertex functions that depend on the momentum transfer between ^{3}He and ^{4}He density fluctuations. The model is clearly concocted to make density excitations simple to calculate and illustrations of calculations of single-fermion properties are relegated to Appendix A. The model also does not allow for new "bare" density modes at short wavelengths other than those extrapolated from the QHD regime. There exist now no indications that new modes would appear in the short-wavelength regime, i.e., of the order of k_4. Thus the present model should be useful in analyzing long- and short-wavelength density phenomena in dilute solutions of ^{3}He in ^{4}He.

2.2. The Approximation and Phonon Spectrum

The quantity of interest in the present model calculations is the phonon spectrum $\omega(k)$, which can be obtained from the poles of the retarded density–density propagator, i.e.,

$$\begin{aligned} D_0^{-1}[k, \omega(k)] - \Sigma^R[k, \omega(k)] &= 0 \\ D_0(k, \omega) &= n_4(\hbar k^2/m_4)[\omega^2 - \omega_0^2(k)]^{-1} \end{aligned} \tag{2}$$

where $\omega_0(k)$ is the ^{4}He phonon spectrum, $\Sigma^R(k, \omega)$ is the exact retarded phonon polarization, and the notation follows I. If we assume that the phonon shifts $\delta\omega(k)$ are small, i.e.,

$$\delta\omega(k) \equiv \omega(k) - \omega_0(k), \qquad |\delta\omega(k)| \ll 2\omega_0(k) \tag{3}$$

then we find from (2)

$$\delta\omega(k) = n_4[\hbar k^2/2m_4\omega_0(k)]\Sigma^R[k, \omega_0(k)] \tag{4}$$

The approximation for Σ^R that we use here is the same as that in I, namely Σ^R is approximated by a Hartree term and a second-order one-loop polarization term Π^{0R} as represented by Fig. 7 of I. There exists no exchange Hartree diagram since the phonon polarization diagrams involve mixed external vertices. The approximate Σ^R can be written as [see I, (13d)]

$$\Sigma^R[k, \omega_0(k)] = \gamma^2(k)[2m_4\omega_0(k)/n_4^2\hbar^2k^2]\Pi^{0R}[k, \omega_0(k)] + O(x) \tag{5}$$

where the effective vertex function $\gamma(k)$ is defined as

$$\gamma(k) = n_4[\hbar k^2/2m_4\omega_0(k)]^{1/2}[\gamma_\rho(k) + \omega_0^2(k)k^{-2}\gamma_J(k)] \tag{6}$$

The terms in (5) that are $O(x)$ are the contributions from the first-order Hartree diagrams in Fig. 7 of I. In the event that only the first term in (5) is important, (4) and (5) can be combined to give the phonon shift (real and imaginary parts)

$$\hbar\,\delta\omega(k) = \gamma^2(k)n_4^{-1}\,\mathrm{Re}\,\Pi^{0R}[k, \omega_0(k)] \tag{7a}$$

$$\hbar\,\mathrm{Im}\,\omega(k) = \gamma^2(k)n_4^{-1}\,\mathrm{Im}\,\Pi^{0R}[k, \omega_0(k)] \tag{7b}$$

The one-loop polarization Π^{0R} is given by

$$\Pi^{0R}(k, \omega) = \frac{2}{(2\pi)^3\hbar}\int d^3k'\, n_{k'}^0\left[\frac{1}{\omega - \omega_{\mathbf{k}\mathbf{k}'} + i\eta} - \frac{1}{\omega + \omega_{\mathbf{k}\mathbf{k}'} + i\eta}\right] \tag{8}$$

where $n_k^0 = [e^{\beta(\varepsilon_k - \mu)} + 1]^{-1}$ is the Fermi distribution function, $\omega_{\mathbf{k}\mathbf{k}'}$ is the quasiparticle–hole continuous spectrum

$$\hbar\omega_{\mathbf{k}\mathbf{k}'} \equiv \varepsilon_{\mathbf{k}+\mathbf{k}'} - \varepsilon_{\mathbf{k}'} \tag{9}$$

and ε_k is the $x = 0$ ^{3}He quasiparticle spectrum.

In the next two sections the phonon shift $\delta\omega(k)$ will be calculated for specific examples of ε_k, intersecting or nonintersecting, and for two limiting cases of n_k^0, zero temperature or high temperatures.

3. CALCULATION WITH INTERSECTING BARE SPECTRA

In this section we calculate the shift of the phonon spectrum at $T = 0$ and $T \gg T_F$ under the assumption that the bare ^{3}He quasiparticle spectrum intersects the bare ^{4}He phonon spectrum at some crossover wave vector k_c. We pay particular attention to the shifts at wave vectors near k_c since interesting momentum and temperature dependences are thereby obtained. The use of an effective interaction Hamiltonian (1) with renormalized frequency-independent vertices together with the approximation (Fig. 7 of I) to the phonon polarization Σ^R appears to be well justified in this region of k space. This may be seen by examining low-order corrections to an "unrenormalized" three-point vertex. It is found that at wave vectors near k_c the contributions of such vertex corrections to the real part of the proper self-energy are approximately given by functions of k multiplied by the lowest-order self-energy diagram. This is a consequence of the confinement of the quasiparticle–hole continuum to a small region of (k, ω) space, of the enhancement of specific terms with vanishing energy denominators near k_c, and of the assumed small shift in the phonon spectrum. Further details are given in

Appendix B. The net result of vertex corrections then is to yield a phonon polarization identical in form to that obtained by the use of the effective interaction Hamiltonian (1) in the present approximation.

3.1. Zero Temperature

An interesting feature of the phonon shift at $T = 0$ with intersecting bare spectra is the existence of a maximum and a minimum which straddle the crossover wave vector k_c. As an illustration, we present now a simple calculation utilizing the ^{3}He quasiparticle spectrum ε_k used in I

$$\varepsilon(k) \equiv \varepsilon_k - \varepsilon_0 = \hbar^2 k^2/2m + \cdots \tag{10}$$

where m is an effective mass and k_c is near k_4, e.g., see Fig. 1 of I. It will be shown that $\mathrm{Re}\,\Pi^{0R} \sim O(x^{2/3})$; thus we can use (7a) to calculate the (real) phonon shift. Near k_c, Π^{0R} is dominated by the first term in (8) and $\mathrm{Re}\,\Pi^{0R}$ can be evaluated using (10) to get

$$\mathrm{Re}\,\Pi^{0R}[k, \omega_0(k)] = \frac{2mk_F}{4\pi^2\hbar^2}\left\{\frac{\Delta v}{q^2} + \frac{1}{2q}\left[1 - \left(\frac{\Delta v}{q}\right)^2\right]\ln\left|\frac{1 + \Delta v/q}{1 - \Delta v/q}\right|\right\} \tag{11a}$$

$$\approx \frac{2mk_F}{4\pi^2\hbar^2}\left\{2\frac{\Delta v}{q^2} - \frac{2}{3}\frac{\Delta v^3}{q^4} + \cdots\right\}; \qquad \Delta v \ll q \tag{11b}$$

In (11b) the brace has been expanded in terms of $\Delta v/q$, where $\Delta v \equiv m\,\Delta\omega/\hbar k_F^2$, $q \equiv k/k_F$, and $\Delta\omega$ is the difference between the ^{4}He phonon spectrum and the ^{3}He quasiparticle spectrum

$$\hbar\,\Delta\omega(k) \equiv \hbar\omega_0(k) - \varepsilon(k) \tag{12}$$

which vanishes by definition at k_c. Estimates of the positions of extrema in the phonon shifts $\delta\omega(k)$ can be obtained by substituting the series (11b) truncated at the second term into (7a) and differentiating, assuming that, relative to Δv, q is roughly constant near k_c. We find that near k_c the largest shifts occur roughly at $\Delta v = \pm q$ or

$$\Delta\omega = \Delta\omega_\pm \equiv \pm\hbar k_c k_F/m \sim O(x^{1/3}) \tag{13}$$

i.e., at approximately the entry of the ^{4}He phonon spectrum into the quasiparticle–hole continuum. Since the extrema occur at the limit of convergence for the series (11b), the estimates are rather crude, as can be seen from the numerical determination of $\delta\omega(k)$ given in Section 5 (see Fig. 5).

To estimate the extrema in $\delta\omega(k)$, we evaluate $\mathrm{Re}\,\Pi^{0R}$ at the estimated positions of the extrema $\Delta v = \pm q$. From (11), we find to leading order in x

$$\mathrm{Re}\,\Pi^{0R} \approx \tfrac{3}{2}n_4 x/(\hbar\,\Delta\omega_\pm) \tag{14}$$

and $\mathrm{Re}\,\Pi^{0R} \sim O(x^{2/3})$ as claimed. Substituting (14) into (7a), we find an

estimate of the extrema in $\delta\omega(k)$ to leading order in x

$$\hbar\,\delta\omega_\pm \approx \tfrac{3}{2}\gamma^2(k)x/(\hbar\,\Delta\omega_\pm) \sim O(x^{2/3}) \tag{15}$$

The maximum phonon shift $\delta\omega_+$ is at the low-k side of k_c, whereas the minimum $\delta\omega_-$ is at the high-k side of k_c. Although the spectrum (10) is used explicitly to evaluate (11a), the expansion (11b) and the steps thereafter to (15) are relatively insensitive to the particular form of ε_k but depend essentially on the existence of a crossover wave vector k_c at which point Δv vanishes. Thus the presence of extrema in $\delta\omega(k)$ that straddle k_c can be considered a general feature of the $T = 0$ phonon shift for the case of intersecting bare spectra.

From (7b), we note that the phonon spectrum acquires an imaginary part, the maximum of which is $O(x^{2/3})$, whenever the phonon spectrum is imbedded in the quasiparticle–hole continuum. Hence the phonon shift (real and imaginary parts) at $T = 0$ is $O(x^{2/3})$. This is to be contrasted with the strong coupling case treated in I, where the splitting near k_c resulted in two distinct branches outside the quasiparticle–hole continuum and $\delta\omega(k) \sim O(x^{1/2})$.

3.2. High Temperature $T \gg T_F$

We now consider the high-temperature regime $T \gg T_F$, for which the quasiparticles are distributed according to a Boltzmann distribution. (Note that for the solution in Ref. 5, $T_F \approx 0.3$ K.) We find that to leading order in x the phonon shift is now $O(x)$, in contrast to $T = 0$, where $\delta\omega(k) \sim O(x^{2/3})$. The direct Hartree contributions to Σ^R cannot be ignored in (5) and are given by [see I, (13d)]

$$\{g_\rho(k) - [\gamma_J^2(k)m^{-1} - g_J(k)]\omega_0^2(k)k^{-2}\}n_4 x \tag{16}$$

However, if the combination of vertex functions in (16) is not strongly k dependent near k_c, this contribution is simply a constant shift for k's near k_c. Thus the interesting contribution to the phonon shift still arises from the second-order polarization term in (5) and $\delta\omega(k)$ can be calculated from (7a). Near k_c the dominant part of Re Π^{OR} can be evaluated using (10) in (8),

$$\text{Re}\,\Pi^{OR}(k, \omega_0(k)) = n_4 x\hbar^{-1}k^{-1}(\beta m/2)^{1/2}\Phi([\beta m/2]^{1/2}\,\Delta\omega/k) \tag{17}$$

where $\beta = (k_B T)^{-1}$, k_B is Boltzmann's constant, and $\Phi(z)$ is defined by

$$\Phi(z) \equiv \pi^{-1/2} P \int_{-\infty}^{\infty} dy\,(z - y)^{-1} \exp(-y^2) \tag{18a}$$

$$\approx 2z(1 - \tfrac{2}{3}z^2 + \cdots), \qquad z \ll 1 \tag{18b}$$

$$\approx z^{-1}(1 + \tfrac{1}{2}z^{-2} + \cdots), \qquad z \gg 1 \tag{18c}$$

We further expand (17) using (18b) to obtain

$$\text{Re}\,\Pi^{0R}(k, \omega_0(k)) = n_4 x \hbar^{-1} k^{-2} \beta m(\Delta\omega)[1 - \tfrac{1}{3}\beta m(\Delta\omega/k)^2 + \cdots] \quad (19)$$

From the series (19) truncated at the second term, the positions of the extrema in $\delta\omega(k)$ can be estimated to be

$$\hbar\,\Delta\omega = \hbar\,\Delta\omega_{\pm} \equiv \pm[2\varepsilon(k_c)k_B T]^{1/2} \quad (20)$$

which is approximately the width of the quasiparticle–hole continuum and is well within the convergence limit of (19). Substituting (20) into (19) and (7a), we find the extrema in $\delta\omega(k)$

$$\hbar\,\delta\omega_{\pm} = \tfrac{2}{3}\gamma^2(k)x[2\varepsilon(k_c)k_B T]^{-1/2} \quad (21)$$

As the temperature is increased, the extrema are enhanced as $T^{-1/2}$, which is due to the narrowing of the width (20) of the quasiparticle–hole continuum.

To interpolate between the two limits $T = 0$ and $T \gg T_F$, we note that in both limits the extrema in $\delta\omega(k)$ can be written as

$$\hbar\,\delta\omega_{\pm} \propto \gamma^2(k)x/(\hbar\,\Delta\omega_{\pm}) \quad (22)$$

where the constant of proportionality is of the order of unity. Thus over a wide range in temperature the extrema (22) can be interpreted in terms of the width $\Delta\omega_{\pm}$ of the quasiparticle–hole continuum. As T decreases, $\Delta\omega_{\pm}$ decreases as $T^{1/2}$ and $\delta\omega_{\pm}$ increases as $T^{-1/2}$. As T is decreased through T_F to zero, the width stops narrowing at $T \approx T_F$ [where from (20) $\Delta\omega_{\pm} \sim O(x^{1/3})$] and the boundary of the quasiparticle–hole continuum begins to sharpen for $T < T_F$; concomitantly $\delta\omega_{\pm}$ ceases to increase as $T^{-1/2}$, bends over at $T \approx T_F$, and saturates for $T < T_F$ at its $T = 0$ value.

From (7b) the increase in the half-width of the phonon spectrum due to ^{3}He can be obtained:

$$\hbar\,\text{Im}\,\omega(k) = -(\pi/2)^{1/2}\gamma^2(k)x|\hbar\,\Delta\omega_{\pm}|^{-1}\exp[-\beta\hbar^2(\Delta\omega)^2/4\varepsilon(k)] \quad (23)$$

The maximum width, which occurs at k_c where $\Delta\omega$ vanishes, is seen to have a temperature dependence similar to $\delta\omega_{\pm}$. Away from this maximum, the width falls off as a Gaussian in $\Delta\omega$.

4. CALCULATION WITH NONINTERSECTING BARE SPECTRA

We investigate here the shift in the phonon spectrum for the case in which the ^{3}He quasiparticle spectrum does not intersect the bare ^{4}He phonon spectrum. As an example, we consider an $x = 0$ ^{3}He quasiparticle

spectrum[6,8] ε_k which is given by (10) in the long-wavelength region but displays a minimum Δ_3 at wave vector k_3 approximately equal to k_4,

$$\begin{aligned}\varepsilon(k) &\equiv \varepsilon_k - \varepsilon_0 \\ &= \Delta_3 + \hbar^2(k - k_3)^2/2\mu_3, \qquad k \approx k_3\end{aligned} \tag{24}$$

Here we take the parameters Δ_3 and μ_3^{-1} to be less than the corresponding ^{4}He roton parameters Δ_4 and μ_4^{-1}.

4.1. Zero Temperature

Unlike the intersecting case, the Re Π^{0R} must be calculated using both terms in (8), since it is no longer clear that the first term will dominate. The crudest approximation, which is useful for some applications, is to ignore the k' dependence in $\omega_{\mathbf{k}\mathbf{k}'}$, in which case Re Π^{0R} is simply

$$\text{Re}\,\Pi^{0R}(k, \omega) = n_4 x\left[\frac{1}{\hbar\omega - \varepsilon(k)} - \frac{1}{\hbar\omega + \varepsilon(k)}\right] \tag{25}$$

To improve on (25), we expand $\omega_{\mathbf{k}\mathbf{k}'}$ in powers of k',

$$\begin{aligned}\hbar\omega_{\mathbf{k}\mathbf{k}'} = \varepsilon(k) - \varepsilon(k') + \frac{1}{k}\frac{d\varepsilon_k}{dk}\mathbf{k}\cdot\mathbf{k}' + \frac{1}{2k^2}\left[\frac{d^2\varepsilon_k}{dk^2} - \frac{1}{k}\frac{d\varepsilon_k}{dk}\right](\mathbf{k}\cdot\mathbf{k}')^2 \\ + \frac{1}{2k^2}\frac{d\varepsilon_k}{dk}k'^2 + O(k'^3)\end{aligned} \tag{26}$$

Since we are mainly interested in the phonon shift near k_3, $\omega_{\mathbf{k}\mathbf{k}'}$, to $O(k'^2)$, can be written

$$\begin{aligned}\hbar\omega_{\mathbf{k}\mathbf{k}'} &= \varepsilon(k) - \varepsilon(k') + \frac{1}{2}\frac{d^2\varepsilon(k)}{dk^2}k'^2\cos^2\theta' \\ &\approx \Delta_3 + \frac{\hbar^2 k'^2}{2\mu_3}\cos^2\theta'\end{aligned} \tag{27}$$

where in the second line we have used (10) for $\varepsilon(k')$ and the fact that $\mu_3 \ll m$. Substituting (27) into (8), we find for $\omega = \omega_0(k)$ and k near k_3

$$\begin{aligned}\text{Re}\,\Pi^{0R} = \frac{\mu_3}{\pi^2\hbar^2}\left(\frac{2\mu_3\,\Delta\omega}{\hbar}\right)^{-1/2}\left\{k_F\left(\frac{2\mu_3\,\Delta\omega}{\hbar}\right)^{1/2}\right. \\ \left. + \frac{1}{2}\left(k_F^2 - \frac{2\mu_3\,\Delta\omega}{\hbar}\right)\ln\left|\frac{k_F + (2\mu_3\,\Delta\omega/\hbar)^{1/2}}{k_F - (2\mu_3\,\Delta\omega/\hbar)^{1/2}}\right|\right\} \\ - n_4 x[\hbar\omega_0(k) + \varepsilon(k)]^{-1}\end{aligned} \tag{28}$$

where for some applications the last term can be ignored, since it is roughly of the order $\hbar(\Delta\omega)/[\hbar\omega_0(k) + \varepsilon(k)]$ down from the first term. Expanding (28), we find from (7a) to leading order in x for k near k_3

$$\hbar\,\delta\omega(k) = \frac{\gamma^2(k)x}{\hbar\,\Delta\omega(k)}\left[1 - \frac{\hbar\,\Delta\omega(k)}{\hbar\omega_0(k) + \varepsilon(k)}\right] + \cdots \tag{29}$$

which corresponds to using the simple form (25). Note that $\delta\omega(k) \sim O(x)$, in contrast to the intersecting case, where $\delta\omega(k) \sim O(x^{2/3})$. Although Re Π^{OR} represents only the contribution from the second-order polarization term in Fig. 7 of I and the direct Hartree term (16) is also $O(x)$, Re Π^{OR} contains the contribution of interest that depends strongly on $\Delta\omega(k)$ and on the temperature. The phonon shift at $k = k_3$, calculated from (28) and (7a), is plotted in Fig. 1 as a function of x, using[8] $\Delta_3 = 5$ K, $k_3 = 1.9$ Å^{-1}, $\mu_3 = 0.3m_4$, and taking for the sake of illustration $\gamma(k_3) = 7$ K.

4.2. High Temperature $T \gg T_F$

At sufficiently high temperatures the distribution function in (8) can be written $n_k^0 \approx e^{-\beta\varepsilon(k)}\, e^{\beta\mu}$, where $e^{\beta\mu}$ satisfies

$$n_4 x = 2e^{\beta\mu}[\lambda_T^{-3} + (\mu_3/m)^{1/2}(k_3^2/\pi\lambda_T)\, e^{-\beta\Delta_3}], \qquad \lambda_T^2 \equiv 2\pi\hbar^2/mk_B T \tag{30}$$

The large-k' ($\approx k_3$) contributions to (8) depend logarithmically upon $(\hbar\omega \pm \Delta_3)$ and are down by $e^{-\beta\Delta_3}$, hence they can be neglected. The major contribution to Re Π^{OR} arises from the small-k' region, in which case (27)

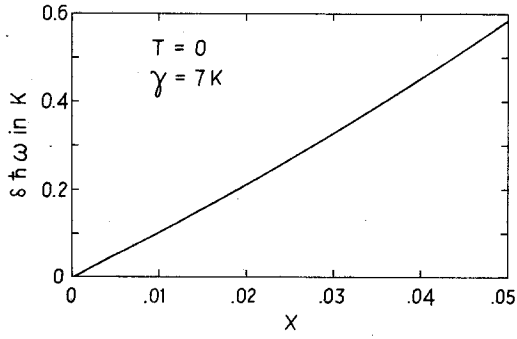

Fig. 1. Calculated phonon shift at the quasiparticle minimum wave vector k_3 and at $T = 0$ as a function of the concentration x assuming nonintersecting bare spectra. For illustration the coupling $\gamma(k_3) = 7$ K has been chosen.

can be used to obtain for $\omega = \omega_0(k)$ and k near k_3

$$\text{Re}\,\Pi^{\text{OR}} = (\pi^{3/2}\beta\hbar^4)^{-1}\mu_3 m\, e^{\beta\mu}(2\mu_3\,\Delta\omega/\hbar)^{-1/2}\Phi([\beta\mu_3\hbar\,\Delta\omega/m]^{1/2}) - 2\lambda_T^{-3}\, e^{\beta\mu}[\hbar\omega_0(k) + \varepsilon(k)]^{-1} \tag{31}$$

where $\Phi(z)$ is defined in (18). For large T, (31) can be expanded, and we find from (7a)

$$\hbar\,\delta\omega(k) \approx 2\gamma^2(k)x(\mu_3/m)(k_B T)^{-1} \tag{32}$$

in contrast to the intersecting case, where $\delta\omega(k) \sim T^{-1/2}$. In deriving (32) we have ignored the last term in (31), which from (30) is T independent as $T \to \infty$ for a fixed x. Note that (31) can be used as an interpolation formula for a wide range in temperature since it yields the correct $T = 0$ answer in the limit of $T \to 0$. Hence as the temperature decreases, the phonon shift $\delta\omega(k)$ becomes increasingly more positive as T^{-1}, until $T \approx T_F$, where $\delta\omega(k)$ bends over to its $T \approx 0$ value. This is illustrated in Fig. 2, where the phonon shift at k_3, calculated from (7a) and the first term in (31), is plotted as a function of T, for $x = 0.05$, $\Delta_3 = 5$ K, $k_3 = 1.9$ Å^{-1}, $\mu_3 = 0.3m_4$, and, as an example, $\gamma(k_3) = 7$ K. To recover the point at $x = 0.05$ in Fig. 1, the whole curve in Fig. 2 needs to be shifted downward by -0.08 K corresponding to the contribution of the last term in (31), which was neglected in Fig. 2. Moreover the neglected Hartree term (16) can also shift the whole curve in Fig. 2 up or down. Nevertheless the phonon shift $\delta\omega(k)$ becomes increasingly more positive as the temperature is decreased in the range $T_F \lesssim T$.

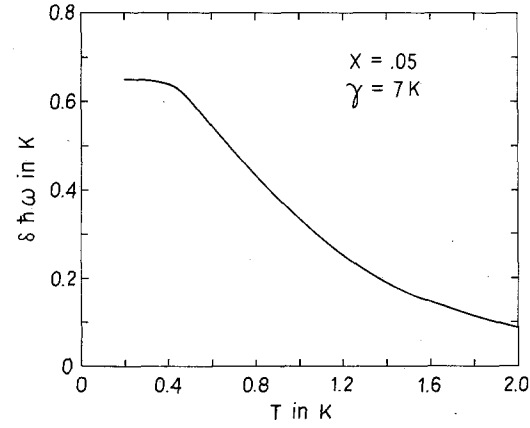

Fig. 2. Calculated phonon shift at $x = 0.05$ and at the quasiparticle minimum wave vector k_3 as a function of the temperature T assuming nonintersecting bare spectra. For illustration the coupling $\gamma(k_3) = 7$ K has been chosen.

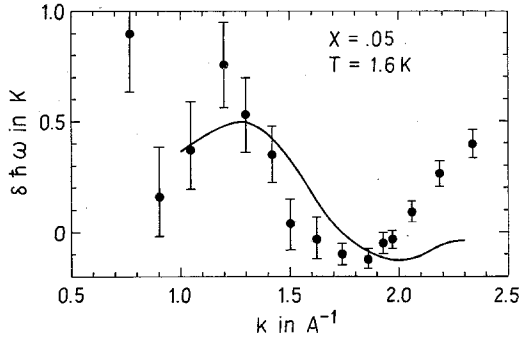

Fig. 3. Measured phonon shift at $x = 0.05$ and $T = 1.6$ K as a function of the wave vector k, and a one-parameter fit assuming intersecting bare spectra. Solid circles represent the data from neutron scattering.[5] Continuous curve represents a calculated one-parameter fit assuming intersecting bare spectra.

5. THEORY AND EXPERIMENT

In this section we consider the existing scattering data[3–5] and suggest further experimentation which should be able to determine the qualitative features of the large-momentum ^{3}He quasiparticle spectrum, as well as to unravel partly the contributions of the various vertex functions to the phonon shifts.

Since neutron scattering appears to be the most direct probe of the low-lying excitations in the ^{3}He–^{4}He system, and since the momentum dependence of the excitation energies is thereby obtained, we concentrate on the experiment of Ref. 5. In Figs. 3 and 4 the solid circles depict the experimental

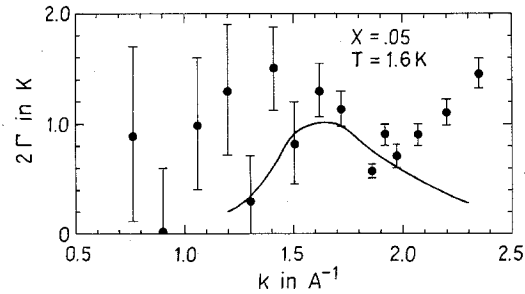

Fig. 4. Measured phonon width increase 2Γ at $x = 0.05$ and $T = 1.6$ K as a function of the wave vector k, and a one-parameter fit assuming intersecting bare spectra. Notation and the one parameter used in the fit are the same as in Fig. 3.

phonon spectrum shift and width increase as a function of wave vector k near the ^{4}He roton wave vector k_4, for $x = 0.05$ and $T = 1.6$ K. As is easily seen, the measured phonon shift $\delta\omega(k)$ attains a maximum at $k \approx 1.2$ Å^{-1}, where it is positive, and a minimum at $k \approx 1.8$ Å^{-1}, where $\delta\omega < 0$.

We may attempt to understand this oscillation in the measured $\delta\omega(k)$ by the use of various qualitatively different model inputs. First, the bare ^{3}He quasiparticle spectrum may either intersect or lie below the ^{4}He phonon spectrum in the momentum range of interest. Second, $\delta\omega(k)$ depends upon the four-vertex functions in a complicated manner, and there is considerable leeway as to which vertices, if any, are dominant. Finally, the momentum dependence near k_4 of the vertex functions may or may not be of primary significance.

We consider first the situation in which the bare spectra do not intersect. In this case, it appears that the experimentally observed oscillation in $\delta\omega(k)$ is to be interpreted (within the model) in terms of some kind of oscillation in k of the vertices. Because of the plethora of possible vertex momentum dependences and possible ^{3}He quasiparticle spectra, we do not at present attempt a fit to the experimental data along these lines, although such an endeavor is clearly possible. However, future experimental determination of the temperature dependence of the shift $\delta\omega(k)$ should make such a program meaningful since it should then be possible to sort out the contributions from the different vertices to some extent. This is due to the fact that only the second-order Π^{0R} contributions to the polarization (5) are temperature dependent, with the result that the T-dependent contributions to $\delta\omega(k)$ may be expressed solely in terms of $\gamma(k)$ defined in (6). Furthermore, in accordance with the results of (32) and Fig. 2, if the bare spectra do not intersect, then $\delta\omega(k)$ should become more positive as the temperature is lowered. This behavior, if present, should provide simple experimental evidence for nonintersection.

If, on the other hand, the bare phonon and ^{3}He spectra intersect at some wave vector k_c less than k_4, then the observed oscillation in $\delta\omega(k)$ can be attributed to either (or both) the k variation of the vertex functions or the change in sign upon crossing at k_c of the shift produced by the second-order polarization terms in Fig. 7 of I. Again T-dependent experimental results may be able to untangle the contributions from the various vertices and terms to $\delta\omega(k)$. Furthermore, the results of Section 3 imply that for intersecting spectra $\delta\omega(k)$ should have an oscillating contribution which becomes enhanced as the temperature is decreased. Thus, it is clear that a low-temperature neutron scattering experiment could provide invaluable information as to the qualitative features of the spectra and their interactions.

We proceed now with an explicit demonstration that the measured phonon shift $\delta\omega(k)$ can be understood in terms of nonoscillating (near k_4)

vertex functions and intersecting bare spectra. We emphasize that this is a highly specific explanation of the available experimental results. However, the qualitative features of the calculation clearly illustrate the type of information that T-dependent experiments could provide.

We parametrize the falloff with increasing k of the four-vertex functions from their $k = 0$ values given by QHD in a very simplified manner. We assume that the vertices are scaled down by factors of a function $\beta(k)$ given by

$$\beta(k) = (1 + b^2k^2)^{-1} \tag{33a}$$

according to

$$\begin{aligned} &\gamma_\rho(k) = \beta(k)\gamma_\rho(0), \qquad \gamma_J(k) = \beta(k)\gamma_J(0) \\ &g_\rho(k) \equiv g_\rho(\mathbf{k}, \mathbf{k}) = \beta^2(k)g_\rho(0) \\ &g_J(k) \equiv g_J(\mathbf{k}, \mathbf{k}) = \beta^2(k)g_J(0) \end{aligned} \tag{33b}$$

where the $k = 0$ values of the vertex functions are taken from QHD, and where the constant b is an adjustable parameter. The magnitude of b will be henceforth specified by stating the value that $\gamma(k)$ assumes at the ^{4}He roton wave vector k_4, where $\gamma(k)$ is defined in (6). We further scale down the effect of the ^{4}He density reduction by the presence of ^{3}He atoms by a factor $\beta^2(k)$. The net effect of the scaling down is roughly to reduce by a factor $\beta^2(k)$ all shifts of the phonon spectrum produced by assuming that the vertex functions are constant in momentum space.

Having specified the vertices, and assuming the ^{3}He quasiparticle spectrum depends quadratically upon momentum (10), we calculate $S(k, \omega)$ at $T = 0$ and $T > 0$. [At $T = 0$ we can find the phonon shift by solving (2) numerically.] The solid curve in Fig. 3 depicts the peak in (k, ω) space of $S(k, \omega)$ at $T = 1.6$ K, $x = 0.05$, and for $\gamma(k_4) = 5.5$ K. As can be seen, we obtain semiquantitative agreement with the data of Ref. 5. Variations from the experimental results can be easily attributed to the oversimplification of (33) in describing the momentum dependence of the vertices. Figure 4 shows a comparison between experiment and theory of the width $2\Gamma(k)$ of the peak in $S(k, \omega)$, again at $T = 1.6$ K, $x = 0.05$, $\gamma(k_0) = 5.5$ K. Although theory seems to yield the right order of magnitude for the width, discrepancies with experiment are clear. This is possibly due to our neglect of certain higher order processes, as well as to the fact that the widths are considerably more difficult to ascertain experimentally than the spectrum shifts. In accordance with the results of Section 3, upon lowering the temperature from $T = 1.6$ to 0 K the phonon shift increases as $T^{-1/2}$ [Eq. (21)] and undergoes a transition near $T \approx T_F$ from a linear dependence on x [Eq. (21)] to one of order $x^{2/3}$ [Eq. (15)] at $T = 0$. The phonon shift is thus considerably enhanced as $T \to 0$. In Fig. 5, we compare the calculated phonon shift as a function of k

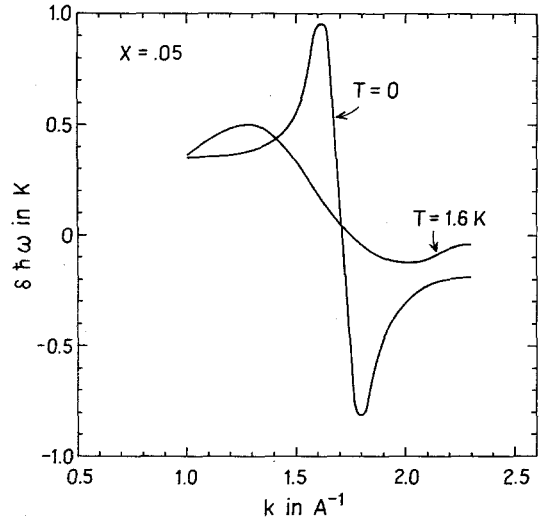

Fig. 5. Calculated phonon shift at $x = 0.05$ as a function of the wave vector for $T = 0$ and $T = 1.6$ K, based on the one-parameter fit to the neutron data (Figs, 3–4). assuming intersecting bare spectra,

at $T = 1.6$ K with that at $T = 0$ K for $x = 0.05$ and $\gamma(k_4) = 5.5$ K. Note both the enhancement of the shift and the lessening of the separation in k space between the extrema of the shift as the temperature is lowered. Clearly the calculated temperature dependence of the phonon shift is of sufficient magnitude as to make experimental confirmation or refutation of this type of theory possible. Note, however, that if part of the experimental oscillation in $\delta\omega(k)$ is due to variation in the vertices as functions of k, then the low-temperature enhancement of $\delta\omega(k)$ should be less than predicted here, although it should have the same qualitative behavior.

We now briefly consider the existing Raman scattering experiments. If the Raman data are to be interpreted with allowance for a two-roton bound state, it may be necessary to take into account the concentration dependence of the binding energy (0.37 K for pure ^{4}He), since the phonon shifts $\delta\omega(k)$ of Figs. 2 and 5 not only displace but also distort the roton minimum. For intersecting (nonintersecting) bare spectra, the $x > 0$ roton mass parameter μ is decreased (increased) and the two-roton binding energy is decreased (increased). Such shifts in the binding energy, while certainly negligible on the scale of the ^{4}He roton energy Δ_4, need not be small in comparison to the phonon shifts $\delta\omega(k)$. A rough estimate of the change in the two-roton binding energy for intersecting bare spectra gives a value of the order of 0.1 K. It should be noticed that direction of the binding energy shift is to compensate

part of the phonon shift $\delta\omega(k)$. If, however, the Raman experiments can be interpreted rigorously as a direct measurement of the energy of pairs of $x > 0$ rotons, then we can compare the existing Raman data at lower ($T = 0.6$ K) temperature with the above theoretical results. From Fig. 5, which is based on a fit to the neutron scattering data assuming intersecting bare spectra, we deduce that the theory gives a much larger phonon shift at $T = 0.6$ K than that ($\ll 0.1$ K) deduced from the Raman data. Although Fig. 2, which is based on nonintersecting bare spectra, also appears to give too large a phonon shift at $T = 0.6$ K, the value of the effective coupling $\gamma(k_3) = 7$ K was chosen simply for illustration and is not based on any experimental fit. Thus $\gamma(k_3)$ in Fig. 2 could be readjusted as desired to give results consistent with those deduced from Raman data. Concomitantly we would have to adjust the k dependences of the vertices to fit the neutron data. Hence there is a hint that intersecting bare spectra may be inconsistent while the nonintersecting spectra need not be. However, until the $x = 0$ ^{3}He quasiparticle spectrum is better known and also until it is clear how to analyze the Raman data, such comparisons can only be preliminary and inconclusive.

We conclude that the existing scattering data are not yet sufficient to distinguish even between the two classes of ^{3}He quasiparticle spectrum, i.e., intersecting or nonintersecting. The present model, although simple, still contains too many unknown parameters and interdependences to give an unambiguous conclusion. Further experiments would clearly help sort things out. From the temperature dependence of the phonon shift characteristic of intersecting or nonintersecting spectra, it appears that a low-temperature ($T \sim T_F$) neutron scattering experiment would provide valuable information about the vertex functions and the qualitative features of the ^{3}He quasiparticle spectrum.

APPENDIX A. $x = 0$ RENORMALIZATION TERMS

As a further illustration of the use of the effective Hamiltonian (1), we consider here the calculation of the leading x dependence of the chemical potential $\varepsilon_0(x)$ and the effective mass $m(x)$ of the ^{3}He quasiparticle. We show that by subtracting out the $x = 0$ renormalization term which is already included in (1), the QHD results for $\varepsilon_0(x)$ and $m(x)$ are recovered.

To facilitate the discussion, we first consider the effective interaction V between ^{3}He quasiparticles as described by the four-point quasiparticle vertex. To lowest order in x, the four-point vertex has two contributions: a direct ^{3}He–^{3}He interaction, which is taken to be

$$V_d(k) = \gamma_d(k), \qquad \gamma_d(k) = (1 + 2\alpha)m_4c_0^2/n_4 \tag{A1}$$

(c_0 is the sound speed in pure ^{4}He and notation follows I), and the phonon-

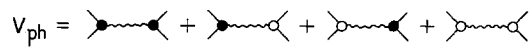

Fig. 6. Diagrammatic representation of the phonon-induced contribution V_{ph} to the effective interaction between ^{3}He quasiparticles.

induced interaction $V_{\rm ph}$, which is given by Fig. 6. A straightforward calculation[15] gives

$$V_{\rm ph} = (n_4k^2/m_4)(\omega^2 - c_0^2k^2)^{-1}\{\gamma_\rho^2 + (\hbar\omega/2mk^2)\gamma_\rho\gamma_J(2\mathbf{p}' + \mathbf{k})\cdot\mathbf{k} + (\hbar\omega/2mk^2)\gamma_\rho\gamma_J(2\mathbf{p} - \mathbf{k})\cdot\mathbf{k} + (\hbar c_0/2mk)^2\gamma_J^2[(2\mathbf{p}' + \mathbf{k})\cdot\mathbf{k}][(2\mathbf{p} - \mathbf{k})\cdot\mathbf{k}]\} \tag{A2}$$

where $\mathbf{p}$ and $\mathbf{p}'$ are the momenta of the incoming ^{3}He quasiparticles. On the energy shell $\omega = \mathbf{k}\cdot(\mathbf{p} - \frac{1}{2}\mathbf{k})/m = \mathbf{k}\cdot(\mathbf{p}' + \frac{1}{2}\mathbf{k})/m$ and in the static limit $\omega \ll kc_0$, we find

$$V_{\rm ph}(k) = (n_4/m_4)[-\gamma_\rho^2c_0^{-2} - (\hbar/m)^2(\gamma_\rho c_0^{-2} + \gamma_J)^2(\mathbf{p}\cdot\hat{\mathbf{k}})(\mathbf{p}'\cdot\hat{\mathbf{k}})] \tag{A3}$$

which is in agreement with the QHD model if the expressions (5) of I are substituted for γ_ρ and γ_J. In the long-wavelength limit, the total four-point vertex is given by

$$V(k) = \gamma_d(k) - (n_4/m_4c_0^2)\gamma_\rho^2(k) \tag{A4}$$

We now calculate the ^{3}He self-energy using the effective Hamiltonian (1) and determine the long-wavelength, x-dependent quasiparticle spectrum as a functional of $V(k)$ given in (A4). We first add a term to (1) that would describe the direct ^{3}He–^{3}He interaction, i.e.,

$$\int d^3x \int d^3x'\gamma_d(\mathbf{x} - \mathbf{x}')\rho_3(\mathbf{x}, t)\rho_3(\mathbf{x}', t) \tag{A5}$$

where $\gamma_d(\mathbf{x} - \mathbf{x}')$ is the Fourier transform of $\gamma_d(k)$. Representing the direct interaction by a dashed line, the ^{3}He self-energy Σ_3 can be represented by the diagrams in Fig. 7. The Hartree term can be easily shown to yield $n_4x\gamma_d(0)$. The exchange term that involves the direct ^{3}He–^{3}He interaction gives straightforwardly $\Sigma_d^{\rm ex} = -\frac{1}{2}n_4x\gamma_d(k)$. However, the last diagram in Fig. 7, which involves a phonon exchange, must be handled carefully. From the Feynman

Fig. 7. Lowest order diagrams for ^{3}He quasiparticle self-energy Σ_3.

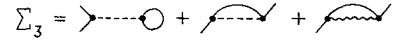

rules[15] we find the contribution

$$\Sigma_{\mathrm{ph}}^{\mathrm{ex}} = -\frac{n_4}{\hbar}\int \frac{d^3k'}{(2\pi)^3}\gamma_\rho^2(k')\frac{\hbar k'}{2m_4c_0} \times \left[-\frac{\theta(|\mathbf{k}+\mathbf{k}'|-k_{\mathrm{F}})}{\omega-\omega_0(k')-\varepsilon_{\mathbf{k}+\mathbf{k}'}/\hbar}+\frac{\theta(k_{\mathrm{F}}-|\mathbf{k}+\mathbf{k}'|)}{-\omega-\omega_0(k')+\varepsilon_{\mathbf{k}+\mathbf{k}'}/\hbar}\right]$$

$$= -\frac{n_4}{\hbar}\int \frac{d3^3k'}{(2\pi)^3}\gamma_\rho^2(k')\frac{\hbar k'}{2m_4c_0} \times \left[\frac{\theta(k_{\mathrm{F}}-|\mathbf{k}+\mathbf{k}'|)}{\omega-\omega_0(k')-\varepsilon_{\mathbf{k}+\mathbf{k}'}/\hbar}+\frac{\theta(k_{\mathrm{F}}-|\mathbf{k}+\mathbf{k}'|)}{-\omega-\omega_0(k')+\varepsilon_{\mathbf{k}+\mathbf{k}'}/\hbar} - \frac{1}{\omega-\omega_0(k')-\varepsilon_{\mathbf{k}+\mathbf{k}'}/\hbar}\right] \tag{A6}$$

In the limit of $x \to 0$ or $k_{\mathrm{F}} \to 0$, $\Sigma_{\mathrm{ph}}^{\mathrm{ex}}$ has a nonvanishing contribution from the last term in the brackets of (A6). This last term must be discarded since it has been included in the definition of the $x = 0$ ^{3}He quasiparticle spectrum. Throwing the $x = 0$ renormalization term out, we change variables, expand in powers of k_{F}, evaluate at $\omega = \varepsilon_k/\hbar$, and take the long-wavelength limit, to get

$$\Sigma_{\mathrm{ph}}^{\mathrm{ex}}(k) = \tfrac{1}{2}n_4x(n_4/m_4c_0^2)\gamma_\rho^2(k) + \cdots \tag{A7}$$

We thereby obtain the ^{3}He self-energy $\Sigma_3(k)$ in the long-wavelength limit to leading order in x

$$\Sigma_3(k) = n_4x[\gamma_d(0) - \tfrac{1}{2}\gamma_d(k) + (n_4/2m_4c_0^2)\gamma_\rho^2(k)] \tag{A8}$$

The $x > 0$ ^{3}He quasiparticle spectrum is given by $\hbar\omega = \varepsilon_k + \Sigma_3(k)$, where ε_k, given in (10), is evaluated at the reduced solution density $n_4 + \delta n_4 = n_4[1 - (1 + \alpha)x]$. Expanding $\varepsilon_0(n_4 + \delta n_4)$, we find to leading order in x

$$\varepsilon_0(n_4 + \delta n_4) = \varepsilon_0(n_4) - n_4x(n_4/m_4c_0^2)\gamma_\rho^2(0) \tag{A9}$$

Defining the x-dependent ^{3}He quasiparticle spectrum by $\delta\varepsilon_k \equiv \hbar\omega - \varepsilon_0(n_4)$, we find from (A8) and (A9) the desired result

$$\delta\varepsilon_k = n_4x[V(0) - \tfrac{1}{2}V(k)] \tag{A10a}$$

Making an explicit expansion of (A10a) in powers of k, we find in agreement with QHD results[10]

$$\delta\varepsilon_k = \delta\varepsilon_0 + [\hbar^2k^2/2(m + \delta m)] + \cdots$$

$$\delta\varepsilon_0 = \tfrac{1}{2}n_4xV(0), \qquad \delta m = \tfrac{1}{2}n_4x(m/\hbar)^2V''(0) \tag{A10b}$$

where $V''(0) = [d^2V(k)/dk^2]_{k=0}$.

The subtraction of the $x = 0$ renormalization term from the ^{3}He self-energy can be understood quite generally by considering first the microscopic one-particle Green's function g and the associated self energy σ, which describe the propagation of the ^{3}He *atoms*, not the quasiparticles. In a solution with a finite concentration x of ^{3}He atoms, the Green's function g_x for the ^{3}He atoms satisfies the Dyson equation

$$g_x = g^{(0)}[1 + \sigma_x g_x] \tag{A11}$$

where $g^{(0)}$ is the Green's function for the propagation of free ^{3}He atoms and σ_x is the self-energy at finite x. As $x \to 0$, (A11) becomes

$$g_0 = g^{(0)}[1 + \sigma_0 g_0] \tag{A12}$$

where g_0 and σ_0 are associated with the propagation of a single ^{3}He atom dissolved in (and interacting with) the liquid ^{4}He. Eliminating $g^{(0)}$ from (A11) and (A12) so as to express g_x in terms of g_0, we find

$$g_x = g_0[1 + (\sigma_x - \sigma_0)g_x] \tag{A13}$$

In order to obtain a description of the system in terms of the *quasiparticle* Green's function with unit spectral weight as used here and in I, we take the quasiparticle Green's function to be given by $G_x = z^{-1}g_x$ near the pole of g_x, where z is the spectral weight of g_x. Writing $\Sigma_x = z\sigma_x$, we obtain from (A13)

$$G_x = G_0[1 + (\Sigma_x - \Sigma_0)G_x] \tag{A14}$$

By absorbing the appropriate factors of z into the effective interaction, we can express Σ_0 as a functional of G_0. Hence (A14) gives a perturbation expansion of the ^{3}He quasiparticle propagator G_x in terms of the $x = 0$ ^{3}He quasiparticle propagator G_0 and displays explicitly the subtraction of the $x = 0$ quasiparticle self-energy.

APPENDIX B. VERTEX CORRECTIONS

In this appendix we examine the effect of vertex corrections on the phonon polarization. We demonstrate that the use of the frequency-independent renormalized vertex functions as given in the effective Hamiltonian (1) is valid in regions of (k, ω) space in which the bare spectra are near each other, as is the case with intersecting spectra for $k \approx k_c$ and $\omega \approx \omega_0(k_c) \equiv \omega_{k_c}$.

We consider the two lowest order diagrams shown in Fig. 8(a,b) in which the vertex here refers to an "unrenormalized" interaction between phonons and ^{3}He quasiparticles. The lowest order diagram (Fig. 8a) is simply $\Pi^0(k, \omega)$ given in (8). The next order diagram (Fig. 8b), denoted by $\Pi^1(k, \omega)$, can be

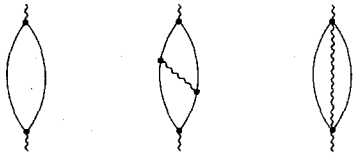

Fig. 8. Various phonon polarization diagrams with (a) no vertex correction, (b) a three-point vertex correction, and (c) the inclusion of four-point mixed vertices. The vertices here are taken to be unrenormalized.

shown to be given by

$$\Pi^1(k,\omega) = \frac{2n_4}{m^4\hbar^2}\int\frac{d^3k'}{(2\pi)^3}\int_{k''<k_F}\frac{d^3k''}{(2\pi)^3}$$

$$\frac{\gamma_u^2(\mathbf{k}''-\mathbf{k}')|\mathbf{k}''-\mathbf{k}'|^2}{\omega_{\mathbf{k}''-\mathbf{k}'}[(\varepsilon_{k''}-\varepsilon_{k'})/\hbar-\omega_{\mathbf{k}''-\mathbf{k}'}]}$$

$$\times\left\{\frac{1}{[\omega-(\varepsilon_{\mathbf{k}+\mathbf{k}''}-\varepsilon_{k''})/\hbar][\omega-\omega_{\mathbf{k}''-\mathbf{k}'}-(\varepsilon_{\mathbf{k}+\mathbf{k}'}-\varepsilon_{k''})/\hbar]}\right.$$

$$\left.+\frac{1}{[\omega+(\varepsilon_{\mathbf{k}+\mathbf{k}''}-\varepsilon_{k''})/\hbar][\omega-\omega_{\mathbf{k}''-\mathbf{k}'}-(\varepsilon_{\mathbf{k}+\mathbf{k}'}-\varepsilon_{k''})/\hbar]}\right\} \tag{B1}$$

where γ_u is the "unrenormalized" vertex function. Keeping only the leading terms in the concentration x and noting that when ω is close to the quasi-particle–hole continuum at $k \gg k_F$ the first term in (B1) has a singularlity and the second term is negligible, we have

$$\Pi^1(k,\omega) \approx -\frac{2n_4}{m_4\hbar^2}\int\frac{d^3k'}{(2\pi)^3}$$

$$\times\frac{\gamma_u^2(k')k'^2}{\omega_{k'}[\omega_{k'}+\varepsilon(k')/\hbar][\omega-\omega_{k'}-\varepsilon(\mathbf{k}+\mathbf{k}')/\hbar]}$$

$$\times\int_{k''<k_F}\frac{d^3k''}{(2\pi)^3}\frac{1}{\omega-[\varepsilon(\mathbf{k}+\mathbf{k}'')-\varepsilon(k'')]/\hbar} \tag{B2}$$

Since the k' integral is a slowly varying function of k and ω, and since the second term in (8) is negligible for ω near the quasi particle–hole continuum at $k \gg k_F$, we have for $\omega \approx \omega_k$,

$$\Pi^1(k,\omega\approx\omega_k) \approx f(k)\Pi^0(k,\omega\approx\omega_k) \tag{B3}$$

where $f(k)$ is given by

$$f(k) \equiv \frac{n_4}{m_4\hbar}\int\frac{d^3k'}{(2\pi)^3}\frac{\gamma_u^2(k')k'^2}{\omega_{k'}[\omega_{k'}+\varepsilon(k')/\hbar][\omega_{k'}-\omega_k+\varepsilon(\mathbf{k}+\mathbf{k}')/\hbar]} \tag{B4}$$

The significant result here is that $\Pi^1(k, \omega)$ given in (B3) is of the same functional form as that obtained by means of the effective Hamiltonian (1), which describes frequency-independent renormalized vertex functions.

The above result can be generalized to any diagram that contains a pair of quasiparticle–hole lines which when cut separate the diagram into two disconnected pieces, i.e., a two-reducible diagram. The introduction of four-point mixed vertices yields diagrams that are not two-reducible, e.g., Fig. 8(c). However, compared with the two-reducible diagrams for ω near the quasiparticle–hole continuum, these two-irreducible diagrams can be neglected. Hence only three-point vertex corrections need be considered, which are in general two-reducible. We conclude that, in regions where the bare spectra are near each other, all three-point vertex corrections can be included in the second-order polarization diagram (Fig. 8a) if we consider the frequency-independent renormalized vertex functions in the effective Hamiltonian (1) as phenomenological parameters to be fitted from experiments.

ACKNOWLEDGMENTS

We acknowledge a number of useful conversions with R. Freeling, D. L. Price, J. Ruvalds, C. M. Surko, and C.-W. Woo.

REFERENCES

1. D. L. Bartley, J. E. Robinson, and V. K. Wong, *J. Low Temp. Phys.* **12**, 71 (1973).
2. T. Soda, in *Low Temperature Physics LT-13* (Proc. 13th Int. Conf. Low Temp. Phys., 1972), R. H. Kropschot and K. D. Timmerhaus, eds. (Plenum, New York, 1974).
3. C. M. Surko and R. E. Slusher, *Phys. Rev. Lett.* **30**, 1111 (1973).
4. R. L. Woerner, D. A. Rockwell, and T. J. Greytak, *Phys. Rev. Lett.* **30**, 1114 (1973).
5. J. M. Rowe, D. L. Price, and G. E. Ostrowski, *Phys. Rev. Lett.* **31**, 510 (1973).
6. L. P. Pitaevski, in U.S.–Soviet Symposium on Condensed Matter, Berkeley, California, May 1973 (to be published).
7. V. I. Sobolev and B. M. Esel'son, *Zh. Eksperim. i Teor. Fiz.* **60**, 240 (1971) [English transl., *Soviet Phys.—JETP* **33**, 132 (1971)].
8. M. J. Stephen and L. Mittag, *Phys. Rev. Lett.* **31**, 923 (1973).
9. A. Bagchi and J. Ruvalds, *Phys. Rev. A* **8**, 1973 (1973); also private communication.
10. J. Bardeen, G. Baym, and D. Pines, *Phys. Rev. Lett.* **17**, 372 (1966); *Phys. Rev.* **156**, 207 (1967).
11. G. Baym, *Phys. Rev. Lett.* **18**, 71 (1967); G. Baym and C. Ebner, *Phys. Rev.* **164**, 235 (1967).
12. W. F. Saam, *Ann. Phys. (N.Y.)* **53**, 219 (1969).
13. R. A. Cowley and A. D. B. Woods, *Can. J. Phys.* **49**, 177 (1971).
14. B. D. Josephson, *Ann. Phys. (N.Y.)* **70**, 229 (1972).
15. D. L. Bartley, Ph.D. Thesis, University of Michigan, 1973 (unpublished).